
IS THERE A LINK BETWEEN PYROLYSIS CONDITIONS AND ADSORPTION CAPACITY OF BIOCHAR?

Bruna Sgarlate^{a,*}, Akel Ferreira Kanaan^a, Marcos Lúcio Corazza^a, Luiz Pereira Ramos^a

^aDepartment of Chemical Engineering, Federal University of Paraná, Av. Cel. Francisco H. dos Santos, 100 - Jardim das Américas, Curitiba- 81530-000, Brazil

*bruna.sgarlate@ufpr.br

Abstract

This study investigates the synthesis and characterization of biochar derived from the slow pyrolysis of industrial digestate (IDT), a byproduct of anaerobic digestion. Biochars were characterized for their water uptake capacity, surface characteristics (BET), and adsorption capacity against model compounds such as methyl violet (MV) and potassium dichromate ($K_2Cr_2O_7$) in aqueous solutions. The results showed that the water uptake capacity was ~38.3% for all tested biochars independent of the pyrolysis processing procedure. A linear relationship between biochar surface area and pyrolysis temperature was attained. Larger surface areas were observed at higher pyrolysis temperature. Biochars presented a mesoporous structure independent of pyrolysis temperature. MV removal efficiency reached 63.9% for C350-22.5 and 74.6% for C550-22.5 at 25 °C. The kinetic data was best described by the pseudo-second order (PSO) model. Biochars had no significant adsorption capacity for $K_2Cr_2O_7$, indicating specificity in their adsorption capabilities. Biochars obtained from pyrolyzed IDT represents a sustainable alternative to the design of sorbent platforms, contributing to improved water quality and resource recovery.

Keywords: Biochar; Adsorption; Thermal conversion; Industrial digestate.

1. Introduction

The ongoing climate crisis threatens the environment with rising global temperatures, increased frequency of extreme weather events, and deteriorating air and water quality [1]. A promising method to mitigate the adverse effects of pollution is adsorption, which effectively captures and removes liquid and gaseous pollutants from the environment [2]. Adsorbents, such as activated carbon, zeolites, and especially biochar, play a crucial role in this process [1,2].

Biochar, a carbon-rich material derived from biomass, can be produced through various thermochemical processes, such as gasification, hydrothermal carbonization, and most notably, pyrolysis. Pyrolysis, especially slow pyrolysis, is favored due to its ability to produce high-quality biochars with enhanced adsorptive properties. For instance, pyrolysis biochars have garnered attention for their ability to adsorb heavy metals and organic contaminants from aqueous streams, and noxious volatiles from gas emissions [3].

This study aims to produce biochar by slow pyrolysis of industrial digestates and evaluate how changes in pyrolysis conditions may affect their surface and structural properties. In addition, we aimed to investigate the adsorption kinetics of model compounds such as methyl violet (MV) and potassium dichromate ($K_2Cr_2O_7$).

2. Methodology

2.1 Materials

Industrial digestate (IDT) (secondary sludge) was obtained from a local sewage company. Samples were dried in an oven at 105°C for 24 h, crushed in a grinder and sieved to generate an average particle diameter of 504 μ m.

2.2 Pyrolysis experiments

The pyrolysis experiments were conducted in a borosilicate tubular reactor (30 \times 8 cm) placed inside a muffle furnace. The pyrolysis temperature varied between 350°C-550°C and the heating rate was in the range of 5-40°C/min. The experimental conditions were determined using a Central Composite Design (CCD) of experiments that was developed using the RStudio software. IDT mass (30 g, dry basis), nitrogen flow rate (20 mL/min), and isothermal retention time (30 min) were kept constants for all experiments. Prior to each experimental run, the reactor was purged with N_2 for 30 min to ensure the absence of oxygen. The mass yield of biochar was determined by calculating the ratio between the mass of the residual material in the reactor and the mass of the initial feedstock.

Biochars were coded according to the temperature and heating rate at which they were obtained (e.g., C380-10 was produced at a

temperature of 380°C and a heating rate of 10°C/min).

2.3 Water uptake capacity of biochar

The water uptake capability of biochar samples was determined via water swelling capacity (WSC) in distilled water (pH = 6.00) at 25°C. Dried samples (0.2g and $d \approx 1.4$ mm) were weighed (m_i) and placed in an Eppendorf microtube. Then, samples were immersed in 1 mL of distilled water. At the end of a 7-day hydration period, samples were weighed (m_f) after carefully removing the excess of water and WSC (%) was calculated according to Eq. (1).

$$WSC (\%) = \frac{m_f - m_i}{m_i} \times 100 \quad (1)$$

Experiments were carried in triplicate and mean values were expressed as $g_{\text{water}}/g_{\text{dried char}}$.

2.4 Surface area and pore size

Biochar surface area was determined using the Brunauer–Emmett–Teller (BET) method and nitrogen adsorption at 77 K. Measurements were made in a BET surface area and pore size distribution analyzer (BEL MicrotracBEL Corp., model Belsorp max, Japan).

2.5 Adsorption experiments

Biochar adsorption capacity was evaluated by employing MV and K_2CrO_7 as model compounds. Briefly, 100 mg biochar was immersed in 10 mL MV or $K_2Cr_2O_7$ solutions (50 $\mu\text{mol/L}$) and sorted at 25°C. The samples were continuously mixed at 100 rpm for 48 h using a Limatec Model LT 600/2 shaker until adsorption reached equilibrium. Aliquots were collected at time intervals and their dye concentration was determined using a Global Analyzer GTA-97 spectrophotometer at 585 nm and 258 nm for MV and $K_2Cr_2O_7$, respectively. The amount of adsorbed contaminant at the desired reaction time (q_t) and adsorption equilibrium (q_e in $\mu\text{mol/g}$) were determined from Eq. (2-3):

$$q_t = \frac{(C_0 - C_t) \times V}{m} \quad (2)$$

$$q_e = \frac{(C_0 - C_e) \times V}{m} \quad (3)$$

where C_0 , C_t and C_e are dye concentrations ($\mu\text{mol/L}$) at the beginning, desired time, and at equilibrium,

respectively, V (L) is the volume of the dye solution, and m (g) is the amount of biochar.

Two different kinetic models were evaluated for their ability to accurately describe the adsorption process. The Pseudo-first order (PFO) and Pseudo-second order (PSO) models are described by Eqs. (4) and (5), respectively.

$$q_t = q_e(1 - e^{(-k_1 t)}) \quad (4)$$

$$q_e = \frac{q_e^2 \cdot k_2 \cdot t}{1 + q_e \cdot k_2 \cdot t} \quad (5)$$

where k_1 and k_2 are PFO and PSO rate constants, respectively.

2.6 Statistical analysis

Statistical analysis of the experimental data was performed by the One-way ANOVA test (statistical significance was considered for p -values < 0.05), followed by a post-ANOVA Tukey test conducted via OriginPro[®]2024b software.

3. Results and discussion

3.1 Water uptake capacity

The water uptake capacity was $\sim 38.3\%$ for all biochars (p -value > 0.05). This result indicates that changes in pyrolysis conditions did not influence biochar water uptake capacity.

3.2 Specific surface area and mean pore size

Specific surface area and average pore diameter of digestate biochars were determined by the BET method (Table 1). Pyrolysis temperature influenced the biochar specific surface area (p -value < 0.05), while the heating rate did not present a significant influence (p -value > 0.05). Biochar specific surface area increased from 6.0 m^2/g to 14.6 m^2/g by increasing pyrolysis temperature from 350°C to 550°C. This increase in surface area can be attributed to the rich organic content of the raw material, which was converted to gaseous products that escaped from the solid material under high temperature, leaving behind a rich porous structure [4]. Furthermore, the average pore diameters reported in Table 1 indicate that the biochars are composed of mesopores (pore size 2.0-50.0 nm) regardless of the pyrolysis temperatures. The large pore structure can enhance adsorption performance

and/or prompt catalytic reaction sites for contaminant removal. These results are similar to those found by Hung [6].

Table 1- Pore properties of biochars

Sample	Surface area (m ² /g)	Mean pore diameter (nm)
C380-10	9.1	13.3
C520-10	14.0	11.6
C380-35	9.6	12.9
C520-35	13.9	12.8
C350-22.5	6.0	16.1
C550-22.5	14.6	12.0
C450-5	10.2	14.1
C450-40	11.7	13.9
C450-22.5 ^{a,b}	14.1 ± 8.1	12.8 ± 2.2

^aData is the mean ± IC (95%)

^b Central point triplicate

The N₂ adsorption-desorption isotherms were determined only for samples C350-22.5 and C550-22.5, which presented the largest and smallest specific surface areas, respectively.

According to Brunauer's classification, the N₂ adsorption-desorption isotherms of digestate biochars (Figure 1) are in accordance to the IV-type curve and the H3 hysteresis loop, which generally occurs in fractured material, accompanied by flat crack structures, cracks and wedge structures. This isotherm shape is characteristic of mesoporous materials where the hysteresis loop (irreversible process) was observed during adsorption-desorption cycle [4].

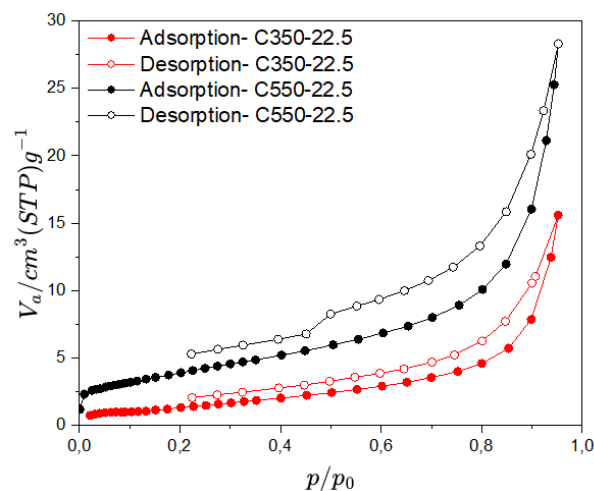
3.3 Kinetics adsorption

Determining the precise timing is crucial for estimating the cost of the adsorption operation. The variation in the amount of adsorbed MV *versus* contact time (0-48 h) is presented in Figure 2. The adsorption tests were performed only for samples C350-22.5 and C550-22.5, which presented the largest and smallest specific surface areas, respectively.

The results indicated that dye adsorption occurred in two phases, with a rapid increase in the initial stage. This rapid increase is attributed to the high number of available free sites for adsorbing dye molecules [6]. Within 5 h, 43.6% (29.17 μmol/g) and 43.1% (29.46 μmol/g) of the total dye

concentration (50 μmol/L) was removed by C350-22.5 and C550-22.5, respectively.

Figure 1- N₂ adsorption/desorption isotherm for C350-22.5 and C550-22.5

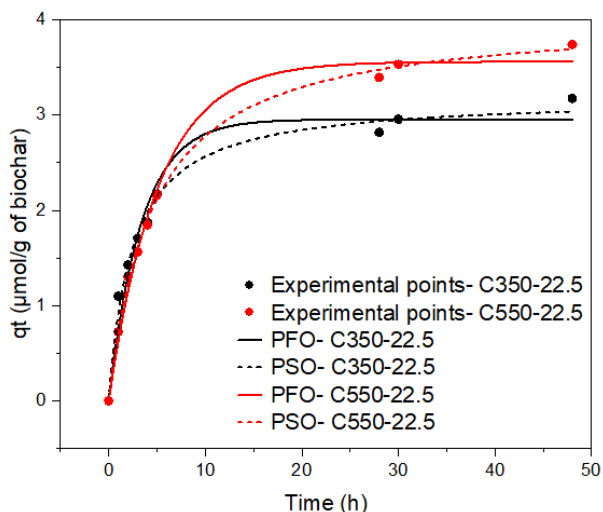


The adsorption capacity increased with agitation time and reached equilibrium at 30 h for both biochars. After 25 h, a gradual decrease in the adsorption rate was observed, where MV ions slowly occupy the remaining active sites due to the saturation of the adsorbent surface [6]. This may also indicate that intraparticle diffusion plays a role in the adsorption process [5]. The percentage of dye removal at equilibrium increased to 63.9% (18.67 μmol/g) and 74.6% (13.13 μmol/g) for the C350-22.5 and C550-22.5 biochars, respectively. From these results, the MV adsorption effectiveness (*p*-value < 0.05) was significantly different between C350-22.5 and C550-22.5.

To define the mechanisms controlling the adsorption interaction between MV molecules and biochar, the kinetic data were treated with two models: pseudo-first order (PFO) and pseudo-second order (PSO). The resulting adsorption parameters are listed in Table 2.

The kinetic data modeling using the PSO model had a better level of agreement with the corresponding experimental data than the PFO model for both samples. The *q_e* values calculated by the model were similar to the experimental data (*q_{e,exp}*), with deviations of 0.31% and 8.02% for C350-22.5 and C550-22.5, respectively.

Figure 2- Effect of stirring time on MV adsorption onto biochar for C350-22.5 and C550-22.5



The poor $K_2Cr_2O_7$ adsorption capacity of digestate biochars demonstrated their selectivity for

MV molecules. In fact, $K_2Cr_2O_7$ concentrations increased as a function of time. We hypothesized that the biochar presented higher affinity for water than for $K_2Cr_2O_7$. As a result, due to their WSC (see section 3.1), adsorption of water molecules from the aqueous media caused an increase $K_2Cr_2O_7$ concentration.

4. Conclusions

In this study, biochars from an industrial digestate (secondary sludge) were produced and characterized. Pyrolysis temperature enhanced biochar surface area, while the rate had no significant influence. Digestate biochars had a high adsorption selectivity for organic dyes such as MV, compared to $K_2Cr_2O_7$. These results indicate that promising biosorbents can be derived from secondary sludge. Valorization of otherwise useless waste materials derived from anaerobic digestion may help promoting a circular bioeconomy in wastewater treatment plants.

Table 2- Parameters of kinetic models

Sample	Kinetic Model	Parameter	Value ^a	p-value	Regression coefficient (R ²)
C350-22.5	Experimental	$q_{e,exp}$ ($\mu\text{mol/g}$)	3.18 ^b	-	-
	PFO	q_e ($\mu\text{mol/g}$)	2.96 ± 0.29	<0.0001	0.966
		k_1 (h^{-1})	0.30 ± 0.09	<0.0001	
	PSO	q_e ($\mu\text{mol/g}$)	3.19 ± 0.21	<0.0001	0.989
k_1 ($\text{g}/\mu\text{mol.h}$)		0.13 ± 0.04	<0.0001		
C550-22.5	Experimental	$q_{e,exp}$ ($\mu\text{mol/g}$)	3.74 ^d	-	-
	PFO	q_e ($\mu\text{mol/g}$)	3.56 ± 0.19	<0.0001	0.992
		k_2 (h^{-1})	0.19 ± 0.03	<0.0001	
	PSO	q_e ($\mu\text{mol/g}$)	4.04 ± 0.12	<0.0001	0.998
k_2 ($\text{g}/\mu\text{mol.h}$)		0.05 ± 0.01	<0.0001		

^aData is the value \pm IC (95%)

^bCalculated by Eq. (3)

References

- [1] Bolan, S. et al. Impacts of climate change on the fate of contaminants through extreme weather events. *Science of the Total Environment*, 168388, 2023.
- [2] Wen, C. et al. Biochar as the effective adsorbent to combustion gaseous pollutants: preparation, activation, functionalization and the adsorption mechanisms. *Progress in Energy and Combustion Science*, v. 99, p. 101098, 2023.
- [3] Ullah, S. et al. Activated carbon derived from biomass

for wastewater treatment: Synthesis, application and future challenges. *Journal of Analytical and Applied Pyrolysis*, 106480, 2024.

[4] Liu, J. et al. Preparation of biochar from food waste digestate: pyrolysis behavior and product properties. *Bioresource technology*, v. 302, p. 122841, 2020.

[5] Hung, C. Y. et al. Characterization of biochar prepared from biogas digestate. *Waste management*, v. 66, p. 53-60, 2017.

[6] Elsharif, K. et al. Adsorption of crystal violet dye onto olive leaves powder: Equilibrium and kinetic studies. *Chemistry International*, v. 7, n. 2, p. 79-89, 2021.